Scilight

Polymer Design for Advanced Applications

https://www.sciltp.com/journals/pdaa

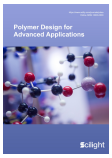

Article

PEDOT-Containing PEG Click-Hydrogel as In Situ Forming Subcutaneous Depot for Electrically-Controlled Insulin Delivery

Helena Muñoz-Galán [1,2], João C. Silva [3,4], Teresa Esteves [3,4], Oscar Bertran [5], Frederico Castelo Ferreira [3,4], Albert Espona-Noguera [2,6], Maria-Pau Ginebra [2,6,7,8], Carlos Alemán [1,2,8,*] and Maria M. Pérez-Madrigal [1,2,*]

[1] Departament d'Enginyeria Química, Campus Diagonal Besòs (EEBE), Universitat Politècnica de Catalunya—BarcelonaTech (UPC), Av. Eduard Maristany 10-14, 08019 Barcelona, Spain
[2] Barcelona Research Center for Multiscale Science and Engineering, Campus Diagonal Besòs (EEBE), Universitat Politècnica de Catalunya, C/Eduard Maristany 10-14, 08019 Barcelona, Spain
[3] iBB—Institute for Bioengineering and Biosciences, Department of Bioengineering, Instituto Superior Técnico—Universidade de Lisboa, Avenida Rovisco Pais 1, 1049-001 Lisboa, Portugal
[4] Associate Laboratory i4HB—Institute for Health and Bioeconomy at Instituto Superior Técnico, Universidade de Lisboa, Avenida Rovisco Pais 1, 1049-001 Lisboa, Portugal
[5] Departament de Física, Escola d'Enginyeria de Telecomunicació i Aeroespacial de Castelldefels (EETAC), Universitat Politècnica de Catalunya—BarcelonaTech (UPC), C/d'Esteve Terradas 7, 08860 Castelldefels, Spain
[6] Biomaterials, Biomechanics and Tissue Engineering Group, Department of Materials Science and Engineering, Universitat Politècnica de Catalunya—BarcelonaTech (UPC), Av. Eduard Maristany 10-14, 08019 Barcelona, Spain
[7] Networking Research Centre of Bioengineering, Biomaterials and Nanomedicine (CIBER-BBN), Institute of Health Carlos III, 28029 Madrid, Spain
[8] Institute for Bioengineering of Catalonia (IBEC), Barcelona Institute of Science and Technology, C/Baldiri Reixac 10-12, 08028 Barcelona, Spain
* Correspondence: carlos.aleman@upc.edu (C.A.); m.mar.perez@upc.edu (M.M.P.-M.)

How To Cite: Muñoz-Galán, H.; Silva, J.C.; Esteves, T.; et al. PEDOT-Containing PEG Click-Hydrogel as In Situ Forming Subcutaneous Depot for Electrically-Controlled Insulin Delivery. *Polymer Design for Advanced Applications* **2025**, *1*(1), 1.

Received: 15 September 2025
Revised: 10 November 2025
Accepted: 22 November 2025
Published: 25 November 2025

Abstract: Managing diabetes is an exhausting and overwhelming task, which has a profound impact in the life of patients. Although insulin (INS) administration has been changing according to the technological developments (infusion sets operated by pumps), patients still have to deal with some inconvenient aspects. Within noninvasive alternatives, injectable in situ forming depots, which are low viscosity injectable polymeric solutions, form a semi-solid polymeric matrix upon injection. If INS is embedded within the matrix, it is feasible to achieve a sustained release, particularly relevant for patients that frequently require INS administration. In this work, we present a click-hydrogel, composed of polyethylene glycol (PEG), as a soft biointerface for INS delivery in which biocompatible poly(3,4-ethylenedioxythiophene) nanoparticles (PEDOT NPs) have been added to act as the conductive element to facilitate the controlled release of INS over an extended period of time through electrochemical stimulation. The suitable features of these electroactive PEG-based hydrogels have been characterized and include non-swellability, mechanical robustness, stability in an aqueous environment under physiological conditions, excellent cytocompatibility (86% ± 5% viability of L-929 fibroblasts) and straightforward fabrication, which validate their suitability as an injectable in situ forming depot for INS delivery. Moreover, the electrochemical control over INS release and detection has been verified first in cell culture media and, later, with an ex vivo skin mimic. Positive voltage (+0.6 V) increased INS release by ~70% relative to passive conditions, while negative stimulation (−0.6 V) suppressed its release by ~39%. Overall, our biomaterial represents a promising platform for diabetes management, offering precise temporal control via externally applied electrical inputs.

Keywords: click-hydrogel; PEDOT nanoparticles; insulin delivery; electrical stimulus; bioelectronics

1. Introduction

Diabetes mellitus, which is a metabolic disorder caused by a dysfunction in the body's ability to produce or properly use insulin (INS), has a profound impact in the patient's life from a physical, mental, emotional, and social perspective [1]. Managing diabetes is an exhausting and, especially when raising children, overwhelming task. In the early 1920s, INS was discovered by Banting and Best [2] and, from that moment onwards, diabetes therapy has been changing in line with technological developments.

Since INS is a hydrophilic peptide hormone of approximately 5.8 kDa, for an effective diabetes treatment, its delivery has been limited to minimally invasive procedures, such as subcutaneous injectable methods with infusion sets (tubing, cannulas, and needles) and operated by pumps, which were commercially introduced in the 1970s [3]. Although pumps represent a major improvement with respect to previous medical devices (INS being administered exclusively via syringe with multiple daily injections), diabetic patients still have to deal with some inconvenient aspects, such as cannula maintenance, skin tissue damage and potential infections, or allergic reactions to the adhesive attaching the infusion set to the skin, among others [4].

Within noninvasive approaches, the oral administration of INS minimizes such drawbacks [5,6]. However, the efficiency of delivery is low since the enzymes present in the gastrointestinal fluid inactivate/digest the hormone and, thus, decrease its bioavailability [7]. Alternatively, skin-penetrating transdermal, topical or injectable delivery systems [8,9], which have been designed as microneedles [10], microspheres, in situ forming depots or composite systems [11], avoid the first-pass metabolism, which result in fewer side effects related to the liver and kidney functioning. In addition, these delivery systems are particularly relevant for patients that frequently require INS administration.

To optimize INS delivery, the use of advanced methods based on physical (e.g., electrical currents [12–14], microwave [15], ultrasound [16]) or chemical triggers have been studied with the aim of enhancing the permeability of INS across the lipid-rich stratum corneum (SC) [17], which is the dense lamellar uppermost layer of the skin [18]. For instance, in chemical-based strategies, we find permeation enhancers [19–21], such as ionic liquids, surfactants, fatty acids, esters, amino acids, and peptides, which disrupt the lipid structure of the SC and, in consequence, improve the capacity of INS to diffuse through it [22–24].

The market of digital devices for INS release is evolving towards a more advanced technological approach that mimics the activity of the pancreas. For that, closed-loop systems, which allow for a high dosage precision on INS delivery, as well as accurate reproducibility on glucose detection [25], are needed to infuse INS in a controlled manner, requiring also the components of the devices being biocompatible and ensuring INS stability [26]. Indeed, according to the patient's glucose level in blood, the desired INS concentration (i.e., INS administration dosage) should be determined and released in a smart manner, thus coupling both real-time monitoring and reliable delivery control [27].

Stimuli-responsive hydrogel-based devices have been reported as embedding systems to protect INS during its controlled release via variable electrical stimuli. For instance, chitosan, which is a natural cationic polysaccharide that contains amino groups, stands out as it has been selected on several occasions to tailor the specialized delivery of INS, being manufactured either as hydrogel scaffolds [28,29], nanoparticles [30] or microneedle patches [31]. Other polymers being explored include polyacrylic acid and polymethacrylic acid hydrogels [32], poly-γ-glutamic acid [33], or polyethylene glycol (PEG) [34].

Herein, we present the optimization of an INS-containing PEG click-hydrogel as a soft biointerface for injectable INS delivery in which biocompatible poly(3,4-ethylenedioxythiophene) nanoparticles (PEDOT NPs) act as the conductive element to facilitate the controlled release of INS over an extended period of time through electrochemical stimulation. The suitable features of these electroactive PEG-based hydrogels [34], which include non-swellability, mechanical robustness, stability in aqueous environment under physiological conditions, biocompatibility and straightforward fabrication, validate their suitability as INS delivery systems in advanced digital devices for diabetes management, like wearable real-time INS-sensing devices. Hence, after the complete rheological and cytocompatibility characterization of the PEG-based hydrogels, their dual electrochemical function (INS release and detection) was evaluated first in cell culture media and, later, with an ex vivo skin mimic. Overall, we envision our biomaterial platform to hold promise for fully integrated multisensor-guided closed-loop INS delivery systems, as well as for other relevant bioelectronic applications related to INS therapy, such as disposable test strips.

2. Methodology

2.1. Materials

3,4-Ethylenedioxythiophene (EDOT, 97%), anhydrous lithium perchlorate ($LiClO_4$), ammonium persulfate (APS), dodecyl benzenesulfonic acid (DBSA), ethanol, and bovine insulin (INS) with a purity ≥ 25 USP units/mg and Mw = 5733.49 were obtained from Sigma-Aldrich and used without further purification. PEG precursors were synthesized as previously reported [35]. Screen-printed electrodes were purchased from Metrohm (Drop Sense C110). 0.1 M phosphate buffered saline (PBS) solution was prepared using Milli-Q® water at room temperature (21 °C) (pH = 7.4, 137 mM NaCl, 8 mM Na_2HPO_4, 2 mM KH_2PO_4, and 2.7 mM KCl—all salt reagents needed were purchased from Sigma-Aldrich, St. Louis, MO, USA).

For the in vitro cellular cytocompatibility studies, L-929 mouse fibroblasts were purchased from ATCC (number CCL-1), while low-glucose Dulbecco's modified Eagle's medium (DMEM), fetal bovine serum (FBS) and antibiotic-antimycotic (Anti-Anti) solution were acquired from Gibco, ThermoFisher Scientific (Grand Island NY, USA). The in vitro Toxicology Assay Kit, MTT based (TOX1-1KT) was purchased from Sigma-Aldrich.

2.2. Synthesis of Poly(3,4-ethylenedioxythiophene) Nanoparticles (PEDOT NPs)

PEDOT NPs were synthesized by the oxidative emulsion polymerization of EDOT in an aqueous solution of ethanol (12.5 vol%) [36]. APS was employed as oxidant, whereas DBSA was utilized as an anionic surfactant to facilitate the formation of micelles, as well as doping agent. The reaction was conducted at 40 °C, under stirring (750 rpm), and protected from light. 0.115 g of DBSA were added to 31.7 mL of Milli-Q water (pre-heated at 40 °C) and stirred for 1 h. Then, 144 µL of EDOT were added drop-wise, followed by 4 mL of ethanol. After 1 h of agitation, the solution was finally combined with 4 mL of Milli-Q® water containing 0.7296 g of APS. The reaction proceeded for 16 h until it was allowed to cool down to room temperature (21 °C). The resulting PEDOT NPs were washed by centrifugation at 11,000 rpm and 4 °C for 40 min. After washing, the supernatant was removed and 40 mL of Milli-Q® water were added to the NPs prior sonication for 20 min. Finally, PEDOT NPs were dried under vacuum at room temperature.

2.3. Preparation of Electroactive PEG-Based Click-Hydrogels

PEDOT NPs (12.4 mg) were stabilized (6.2 mg/mL) in 2 mL of 0.1M PBS under stirring for three days at 1000 rpm followed by sonication for 30 min. To 0.5 mL of this suspension, 3-arm or 4-arm PEG precursors functionalized with either thiol (3_S or 4_S) or alkyne moieties (3_A or 4_A) were dissolved separately and vortexed for 60 s. Specifically, 131 mg of 3_S, 120 mg of 3_A, 107 mg of 4_S, and 100 mg of 4_A were used. Then, the thiol- and yne-containing precursor solutions were mixed together (3_S + 3_A or 4_S + 4_A to yield PEDOT-3-clickPEG or PEDOT-4-clickPEG hydrogels, respectively) in a small glass vial and vortexed for 10 s before allowing the system to gel. Hence, the resulting hydrogel was produced with a thiol:alkyne molar ratio of 1:1 and a total PEG precursor concentration of 20 wt%. The term PEDOT-#-clickPEG hydrogel refers to both systems regardless if they derive from the 3- or the 4-arm PEG precursors. To obtain the hydrogel, the glass vial was broken with a hammer by hitting carefully the top part of the vial. The stability of the hydrogels allowed for this procedure without damaging them. Control thiol-yne PEG-based click-hydrogels (#-clickPEG hydrogels) were prepared following the same procedure but using 0.1 M PBS without PEDOT NPs.

2.4. Characterization of Electroactive PEG-Based Click-Hydrogels

The physical characterization of hydrogels, as well as their swelling response, included gel fraction (GF), equilibrium water content (EWC), and swelling factor (SF) parameters. Hydrogels were produced as described and left to cure for 1 h at room temperature (21 °C) before further testing. No washing step was conducted after gelation for any of the three characterization procedures. Accordingly, hydrogels are referred to as prepared, and three independent samples (n = 3) were considered for each test.

Regarding the GF value, as prepared hydrogels were lyophilized and weighted (W_{L1}). Afterwards, the hydrogels were immersed in Milli-Q® water for three days. During this period, several washes per day were performed to clean the medium of solute concentration. After the three days, the rehydration process was finished, and the hydrogels were again lyophilized and weighted (W_{L2}). Then, the GF was calculated according to the following expression:

$$GF(\%) = \frac{W_{L2}}{W_{L1}} \times 100 \quad (1)$$

The EWC corresponds to the amount of water in the swollen hydrogel by weight after 24 h of immersion. As prepared hydrogels were immersed in Milli-Q® water for 24 h and weighted after drying manually the water excess (W_S). Then, hydrogels were lyophilized and weighted again (W_L). The EWC value was calculated according to the following expression:

$$EWC(\%) = \frac{W_s - W_L}{W_S} \times 100 \quad (2)$$

For measuring the SF value, as prepared hydrogels were immersed in PBS and incubated at 37 °C in an orbital shaker incubator at 80 rpm for 10 days. The PBS solution was changed regularly and, at every time point, hydrogels were taken out of the solution, dried carefully, and weighted. The SF value was calculated by applying the following expression:

$$SF(\%) = \frac{W_0}{W_t} \times 100 \quad (3)$$

were W_0 is the initial weight before immersion (as prepared) and W_t is the weight at each specific time point.

To characterize morphological features, a scanning electron microscopy (SEM) was used and operated at 3 kV (Neon40 Crossbeam™ workstation acquired from Carl Zeiss, Oberkochen, Germany) and equipped with a focused ion beam with an energy-dispersive X-ray (EDX) spectroscopy system). To prevent electron charging issues, all samples were sputter-coated with a thin carbon layer using a K950X Turbo Evaporator (FEDELCO, S.L., Madrid, Spain).

Electrochemical characterization was performed using Autolab PGSTAT101 (Metrohm Autolab B.V., Utrech, The Netherlands) by means of cyclic voltammetry (CV). All experiments were run in a 0.1 M PBS solution (pH = 7.4) at 21 °C considering −0.2 V and 1.0 V as initial/final and reversal potentials, respectively, and a scan rate of 50 mV/s. Data was evaluated by using the NOVA v2.1 software (Metrohm Autolab B.V., Utrech, The Netherlands). All characterization assays were performed considering at least three independent samples.

Regarding rheological characterization, the hydrogels were evaluated using a Hybrid Rheometer Discovery HR-2 (TA Instruments—Waters Cromatografía, S.A., Barcelona, Spain)) equipped with a 20 mm parallel plate geometry and a fixed gap of 450 μm. All measurements were conducted at room temperature. Three oscillatory tests were carried out: time sweep, frequency sweep, and amplitude sweep. Additionally, a compression test was performed to assess the mechanical resistance of the hydrogels. To monitor the crosslinking process and determine the gelation point, a time sweep test was performed under constant conditions. The storage modulus (G′) and loss modulus (G″) were recorded over a period of 500 s at a fixed angular frequency of 1 Hz, with a displacement of 1×10^{-3} rad and a delay time of 3 s. After gelation, a frequency sweep test was conducted to evaluate the mechanical stability of the hydrogels. This test was performed at a constant displacement of 1×10^{-3} rad, while the angular frequency was varied from 0.1 Hz to 1000 Hz. G′ and G″ were recorded as a function of frequency. Subsequently, an amplitude sweep test was carried out to assess the structural integrity of the hydrogel network. The sample was subjected to oscillatory shear at a constant frequency of 1 Hz, while the amplitude was progressively increased from 1×10^{-4} rad to 1 rad. The resulting G′ and G″ values were used to determine the critical amplitude at which the hydrogel structure collapses, indicating structural breakdown. Finally, a compression test was performed using the same rheometer equipped with a 50 N load cell. Freshly prepared hydrogel samples were axially compressed between parallel plates, with the upper plate descending at a constant rate of 1 mm/min. The force required to induce a 5% deformation was recorded to evaluate the compressive stiffness and resistance of the hydrogels.

2.5. Molecular Dynamics (MD) Simulations

Molecular models used to simulate the nanostructure of 3-clickPEG and 4-clickPEG consisted on 192 crosslinked chemical repeat units. The empty space of each model was filled with around 176,000 water molecules, and the final molecular models reached more than 600,000 explicit atoms. The models were minimized (Newton Raphson method) relaxing both the polymer and water atoms using the NAMD 2.9 program [37]. The heating and equilibration processes were identical to those described in our previous work [38]. After that, a production trajectory of 50 ns NPT MD at 298 K and 1 bar was performed following an already described protocol [38].

2.6. Cytocompatibility Studies

In vitro cell culture assays were performed using L-929 mouse fibroblasts (ATCC number CCL-1). Cells were thawed from nitrogen cell banks and expanded in low-glucose Dulbecco's modified Eagle's medium (DMEM, Gibco, ThermoFisher Scientific, Grand Island NY, USA) supplemented with 10% *v*/*v* fetal bovine serum (FBS, Gibco, ThermoFisher Scientific) and 1% *v*/*v* antibiotic-antimycotic (Anti-Anti, Gibco, ThermoFisher Scientific) inside an incubator at 37 °C and 5% CO_2. Cells were passaged to new tissue-culture polystyrene (TCPS) flasks when a confluence of 80–90% was reached and the culture medium was fully renewed every 3 days. Before testing the cytocompatibility of PEDOT-4-clickPEG hydrogels by indirect (extract medium) and direct contact test, the hydrogel samples were sterilized through incubation in a 1% *v*/*v* Anti-Anti solution (in PBS) for 3 h at room temperature (one wash every hour). For both tests, the cells were seeded in 24 TCPS-plates at a density of 1.0×10^5 cells/well and cultivated to confluence for 24 h at 37 °C and 5% CO_2. L-929 cells cultured in DMEM + 10% FBS + 1% Anti-Anti culture media under standard conditions were used as negative control and latex was used as a positive control.

For the direct contact assays, disc-shaped hydrogels of 0.45 cm radius and 0.5 cm height were carefully placed on top of the confluent cell monolayer of L-929 fibroblasts (three replicates per condition) and incubated for 72 h at 37 °C and 5% CO_2. Then, the viability and morphology of the L-929 fibroblasts were qualitatively assessed under an inverted optical microscope (LEICA DMI3000B, Leica Microsystems, Wetzlar, Germany) equipped with a digital camera (Nikon DXM1200F, Nikon Instruments Inc., Melville, NY, USA). For the indirect test, medium extracts were prepared by incubating the discs in DMEM + 10%FBS + 1% Anti–Anti culture media at a ratio of 0.2 g/mL for 24 h at 37 °C/5% CO_2, following ISO 10993-5:2009 [39]. Afterwards, the culture media was removed and L-929 cells were exposed to the material extract's conditioned medium for 72 h at 37 °C/5% CO_2. Then, the relative cell viability was quantified by the MTT (3-[4,5-dimethylthiazol-2-yl]-2,5 diphenyl tetrazolium bromide) assay using the In Vitro Toxicology Assay Kit—MTT-based (Sigma-Aldrich) following the manufacturer's instructions. The percentage of viable fibroblasts was calculated by comparison with the values obtained for the negative control. Five independent samples (n = 5) were tested per experimental condition, and the absorbance values of each one were measured in triplicate using a plate reader (Infinite M200 PRO, TECAN, Mannedorf, Switzerland) at 570 nm.

2.7. Preparation of the Devices for INS Delivery by Combining PEDOT NPs and ClickPEG Hydrogels

PEDOT NPs were added to 0.2 mL of 0.1 M PBS and stabilized as previously described. After sonication, 45 mg of INS were added and the suspension was vortexed for a few seconds. Then, 20 µL were drop-casted onto a screen-printed electrode (working electrode, WE) and left to dry at room temperature (21 °C). On top of this layer (NPs+INS), 75 µL of the reactants required to prepare electroactive clickPEG hydrogels (+6.2 mg/mL of PEDOT NPs and 2.25 mg/mL of INS) were drop-casted and let to gel and stabilize for 15 min before the release study. This device configuration is named hereafter as NPs+INS/PEDOT-#-clickPEG hydrogels.

2.8. Electrochemically Driven INS Delivery from NPs+INS/PEDOT-#-clickPEG

After hydrogel formation, the NPs+INS/PEDOT-#-clickPEG devices were divided into three experimental groups (n = 3 per group) to study INS release under different electrical conditions. Each device was immersed in 1 mL of 0.1 M PBS at room temperature (21 °C). In the first group, a constant voltage of +0.6 V was applied for 100 s via chronoamperometry prior to each sampling with an Autolab PGSTAT101 (Metrohm Autolab B.V., Utrech, The Netherlands). In the second group, the same protocol was followed but using –0.6 V. The third group served as the unstimulated control, with no voltage applied at any time. After each stimulation (or incubation in the control group), the PBS medium was removed and analyzed for released INS using cyclic voltammetry (CV). Devices were then transferred to fresh PBS without further treatment until the next time point. This procedure (electrical stimulation followed by solution exchange and CV analysis) was repeated at 5 mi, 30 min, 60 min, 2 h, 24 h, 48 h, and 72 h. Control and blank samples were subjected to the same handling conditions to ensure consistency across all groups.

2.9. Performance of NPs+INS/PEDOT-4-clickPEG with an Ex Vivo Skin Mimic

To evaluate the effect of biological tissue on electrically controlled INS release, a proof-of-concept ex vivo experiment was conducted using chicken skin as a model barrier. The experiment was designed to mimic a transdermal stimulation setup, where electrical signals are applied externally, and the INS-loaded hydrogel is located beneath the skin, as would occur in a subcutaneous injection scenario. A screen-printed electrode (SPE)

was placed at the bottom of an electrochemical cell, followed by the careful placement of a section of chicken skin directly on top. Chicken skin was selected because of its comparable electrical conductance and barrier properties to human skin, as well as its availability, ease of handling, and minimal subcutaneous fat, which allows for more reproducible electrical stimulation conditions. On top of the skin layer, the hydrogel formulation NPs+INS/PEDOT-4-clickPEG was fabricated in situ. The assembled system (SPE-chicken skin-hydrogel) was immersed in 1 mL of 0.1M PBS at room temperature (21 °C). A constant voltage of +0.6 V was applied for 100 s via chronoamperometry prior to each sampling time point. This stimulation protocol was repeated at 5 min, 30 min, 60 min, 2 h, 24 h, 48 h, and 72 h. After each stimulation, the PBS medium was removed and analyzed for INS content using cyclic voltammetry (CV), and the device was replenished with fresh PBS without further treatment until the next stimulation point. No negative voltage or unstimulated control groups were included in this ex vivo experiment, as the primary objective was to assess the shielding (attenuation) effect of the skin on positively charged electrical stimulation and its impact on INS release kinetics. The electrochemical cell setup, handling protocols, and analysis methods were consistent with those used in the experiments described in Section 2.7 to ensure methodological comparability.

3. Results and Discussion

In this study, electroactive PEG-based click-hydrogels have been fine-tuned to be applied as an in situ forming depot for the electrically controlled delivery of INS. Not only is the electrical stimulus expected to control INS release, but also quantify INS concentration by electrochemical sensing, with both processes being feasible thanks to the presence of the conducting polymer PEDOT (Figure 1a). Hence, the dual control displayed by this soft biointerface over INS release and detection, as well as glucose detection [34,40], opens the door to its application as advanced injectable multisensor-guided closed-loop delivery systems.

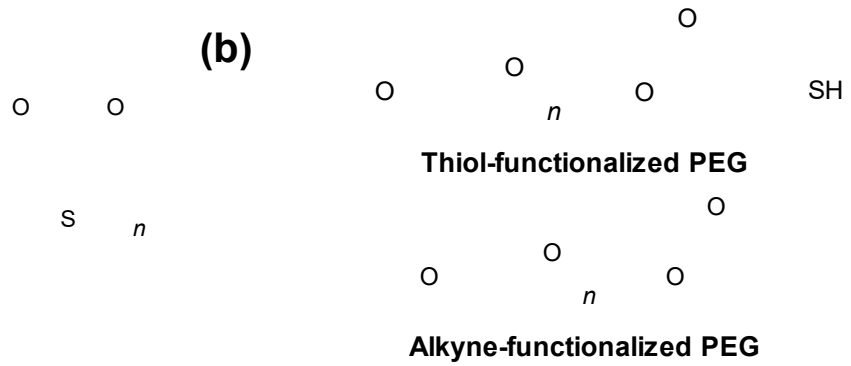

Figure 1. Chemical structure for the materials used for the preparation of PEDOT-#-clickPEG hydrogels: (**a**) PEDOT, as the conducting polymer, and (**b**) thiol- and alkyne-functionalized PEG click-hydrogel precursors.

PEDOT NPs and the PEDOT-#-clickPEG hydrogels were prepared adapting our reported procedures [34,36]. Briefly, 3-arm and 4-arm alkyne- and thiol-functionalized PEG-based moieties (3_A, 3_S, 4_A, and 4_S; Figure 1b) were synthesized by Fischer esterification [35], which represents a straightforward and affordable process, and subsequently mixed in a 1:1 molar ratio of alkyne to thiol polymer precursors at room temperature using PBS solution as solvent and a solids content of 20 wt%, while PEDOT NPs were prepared by oxidative emulsion polymerization and introduced prior to gelation (6.2 mg/mL). In the end, two different systems were obtained: PEDOT-3-clickPEG and PEDOT-4-clickPEG hydrogels resulting from crosslinking 3_A + 3_S and 4_A + 4_S, respectively. The modifications introduced with respect to our previous works [34,36] optimized the properties of our hydrogels in terms of mechanical stability, as well as overall performance to behave as an injectable in situ forming depot. Based on our previous works [34,36], PEDOT NPs have been chosen as conductive moieties, and their use has resulted in electroactive hydrogels (*vide infra*) with minimal disruption of the click chemistry reaction.

For our application, upon injection of the polymeric solution of the PEG precursors, we expect the rapid formation of a solid polymeric network at the injection site. Accordingly, PEG total solid content, which was increased up to 20 wt%, resulted in (i) an even faster gelation (under 30 s by vial tilting method), which takes place in water under mild conditions, with great efficiency and no by-products at all; (ii) higher EWC after 24 h of immersion in PBS at 21 °C; and (iii) long-term stability in the swollen state beyond 20 days under physiological conditions (i.e., pH 7.4 and 37 °C), with an average SF of 104% ± 7% and 89% ± 6% for the PEDOT-3-clickPEG and for the PEDOT-4-clickPEG, respectively, on account of the hydrophobicity of the crosslinking bond. In addition to that, other unique advantages and distinguishing features of our systems include: cytocompatibility,

versatility, which derives from their features being tuneable depending on the manufacturing parameters, for instance PEG precursor used, molecular weight, solid wt%, solvent, thiol to alkyne ration, among other parameters, and excellent robustness—their mechanical features, such as elastic modulus and compressive strength, can be tuned by changing the parameters specified above, thus matching the requirements of the final application.

The gel fraction (GF), which is a well-stablished parameter for assessing the crosslinking of polymeric networks, was determined to be 82% ± 0.3% and 72% ± 2.9%, for 3-clickPEG and 4-clickPEG hydrogels (without PEDOT NPs) respectively, while that of PEDOT-3-clickPEG and PEDOT-4-clickPEG hydrogels were 73% ± 2.3% and 61% ± 1.0%, respectively. Hence, the effect of adding PEDOT NPs during gelation, which decreased the GF values and, thus the efficiency of the thiol-yne crosslinking, was more pronounced for the 4-arm system. Nevertheless, both PEDOT-#-clickPEG hydrogels were mechanically stable and retained their ability to hold water independently of the presence of NPs.

Indeed, the swelling of hydrogels, which is a relevant aspect when considering their application in a biological context, is desirable to be high to ensure a strong resemblance with human tissue and, therefore, their exploitation as drug delivery systems. On the other hand, too much swelling might imply a decrease in the mechanical performance of the hydrogels. In our case, the equilibrium water content (EWC) determined after 24 h for 3-clickPEG and PEDOT-3-clickPEG hydrogels were determined to be 71% ± 0.6% and 73% ± 2.3%, respectively, while for 4-clickPEG and PEDOT-4-clickPEG hydrogels the values were 78% ± 4.9% and 78% ± 1.4%, respectively. As it can be seen, the effect of PEDOT on the EWC was negligible, as the mean values do not show significant difference.

Next, the viscoelastic properties of the PEDOT-#-clickPEG hydrogels were evaluated by rheological characterization (Figure 2). By running time sweeps, the gelation time, which was defined as the sol-gel transition (i.e., instant in which the storage modulus (G′) equals the loss modulus (G″)), was found to be 76 s ± 5.2 s and 45 s ± 8.0 s for PEDOT-3-clickPEG and PEDOT-4-clickPEG hydrogels, respectively. Besides, the end of the crosslinking reaction (i.e., instant in which the G′ plateaus) was observed earlier for the 4-arm hydrogel (ca. 300 s) than for the 3-arm hydrogel (ca. 350 s). Both results correlate well with the fact that the higher the number of arms, the faster the crosslinking reaction and the lower the crosslinking density (by GF determination, *vide supra*). Besides, the G′ moduli, which accounts for the material's ability to store energy elastically under shear, was monitored for both PEDOT-#-clickPEG hydrogels at an amplitude of 1×10^{-3} rad, with the angular frequency varying from 0.1 Hz to 1000 Hz. In all evaluated samples, the G′ modulus was higher than the G″ modulus, which indicates a predominant solid-like behaviour characteristic of crosslinked hydrogels. Regarding the G′ modulus, the G′ value for PEDOT-3-clickPEG hydrogels was higher (12.1 ± 1.8 kPa) than that for PEDOT-4-clickPEG hydrogels by 120% (5.5 ± 1.1 kPa), which we ascribe again to the lower crosslinking density of the latter. Such G′ values remained unaltered when performing amplitude sweep tests until an oscillation displacement of around 0.1 rad was reached, the mechanical stability of both PEDOT-3-clickPEG and PEDOT-4-clickPEG hydrogels being similar. Finally, the required force to cause a 5% deformation by axial compression was 24.3 ± 1.1 N and 20.2 ± 0.5 N for PEDOT-3-clickPEG and PEDOT-4-clickPEG hydrogels, respectively, in good agreement with the much stiffer nature of PEDOT-3-clickPEG hydrogels. Overall, these results indicate an adequate response of the hydrogels under shear, suitable for their application as subcutaneous depot for electrically controlled insulin delivery.

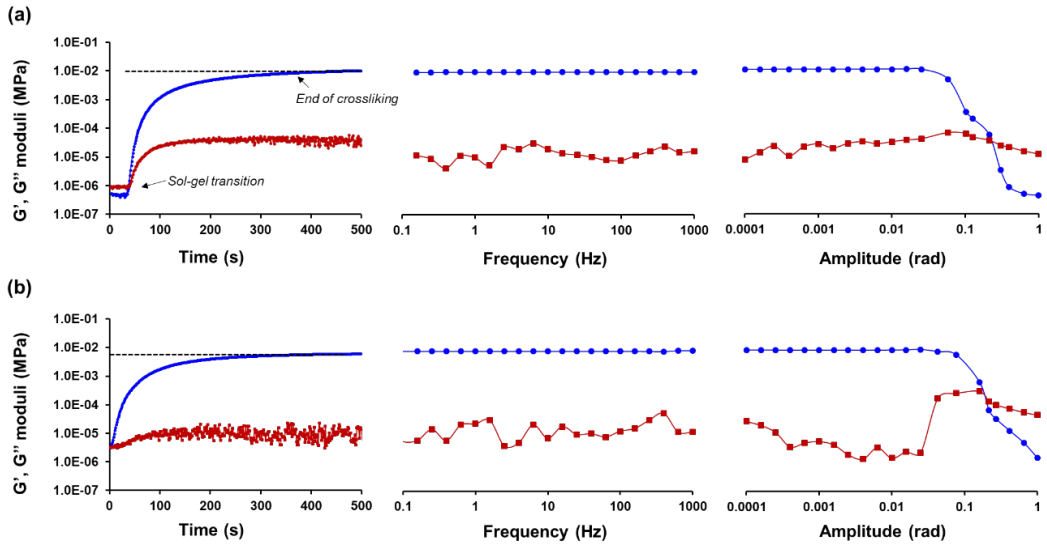

Figure 2. Rheological characterization of PEDOT-#-clickPEG hydrogels. Representative data for (**a**) PEDOT-3-clickPEG and (**b**) PEDOT-4-clickPEG hydrogels: time sweep (**left panel**; hydrogel gelation); frequency sweep

(**middle panel**; hydrogel stability); amplitude sweep (**right panel**; hydrogel breakage). Blue circles and red squares correspond to G′ and G″ moduli, respectively.

Figure 3 displays cross-section SEM micrographs of lyophilized PEDOT-3-clickPEG and PEDOT-4-clickPEG hydrogels. Although both hydrogels are relatively compact, macropores are more detected in the latter than in the former. This porosity is not associated with the intrinsic arrangement of polymer chains but to the macro-structuration of the materials. Indeed, although the 3-arm and 4-arm systems impose some geometrical restrictions in 3-clickPEG and 4-clickPEG hydrogels, respectively, as it was shown by preliminary MD simulations (Figure 3c,d), the resulting nanopores are not visible in the bulk hydrogel. These nanopores, which are similar in size for both hydrogels, remain hidden at the micrometric scale, which may be attributed to the presence of PEDOT or, even, the lyophilization process.

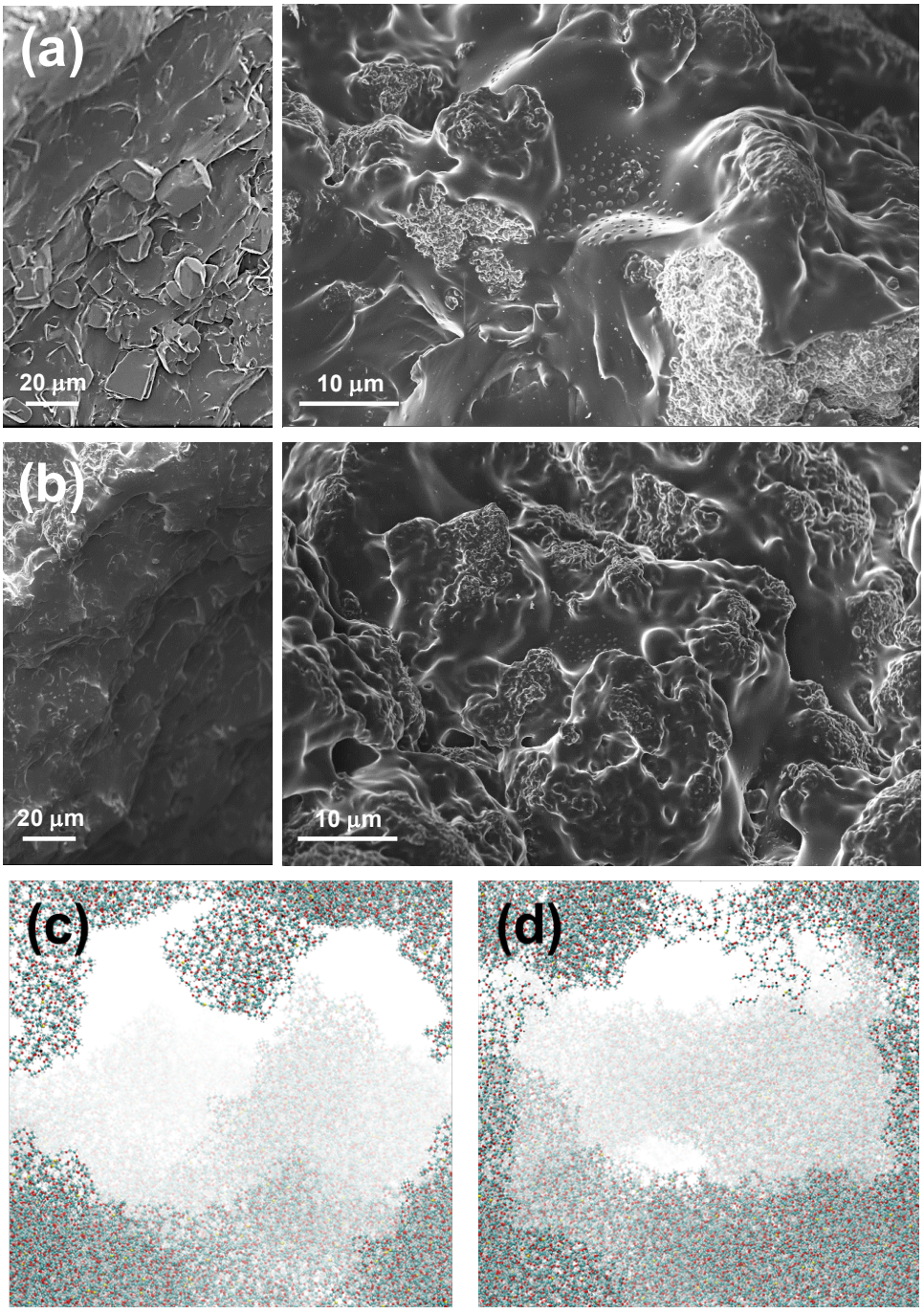

Figure 3. Cross-section SEM micrographs of lyophilized (**a**) PEDOT-3-clickPEG and (**b**) PEDOT-4-clickPEG hydrogels. Last snapshot collected from the production MD runs conducted for (**c**) 3-clickPEG and (**d**) 4-clickPEG, where the length of the simulation box axis is approximately 100 nm.

As we aim to apply our PEDOT-#-clickPEG hydrogels as soft biointerfaces for precisely controlling INS delivery, first, the electrochemical response of PEDOT-3-clickPEG and PEDOT-4-clickPEG hydrogels was determined by cyclic voltammetry (CV, Figure 4a,b). For each system, three CV cycles were run in PBS (pH = 7.4) at room temperature from −0.2 V to 1.0 V (initial/final and reversal potentials, respectively) at 50 mV/s. Comparison between the 3rd cyclic voltammogram recorded for #-clickPEG and PEDOT-#-clickPEG shows an increase in the voltammetry area and the current density because of the redox response of PEDOT NPs, which enhances the electrochemical activity of the blank hydrogel. Specifically, the current density at 1.0 V increases by 692% and 168% for PEDOT-3-clickPEG and PEDOT-4-clickPEG, respectively, when compared to the blank hydrogel. However, it is worth noting that blank hydrogels also displayed some electrochemical activity because of their porous structure, which facilitates the access of electrolyte ions to the electrode. Moreover, the current density is 3.4 times higher for PEDOT-3-clickPEG than for PEDOT-4-clickPEG, which we relate to distribution of the PEDOT NPs within the hydrogel network. Specifically, the conduction mechanism of PEDOT is both electronic (intra- and inter-chain contributions) and ionic. Hence, for PEDOT-#-clickPEG hydrogels to be conductive, a certain degree of percolation between the NPs domains is required, which depends on the porous structure of the hydrogel, as well as PEDOT-PEDOT and PEDOT-PEG interactions. The faster gelation of PEDOT-4-clickPEG hydrogels might impede a uniform dispersion of the PEDOT NPs, thus compromising the interconnectivity between the domains, which eventually affects the electrochemical response of the overall system. Despite this, the presence of PEDOT NPs rendered our PEG-based hydrogels electroresponsive for controlling INS release and quantification.

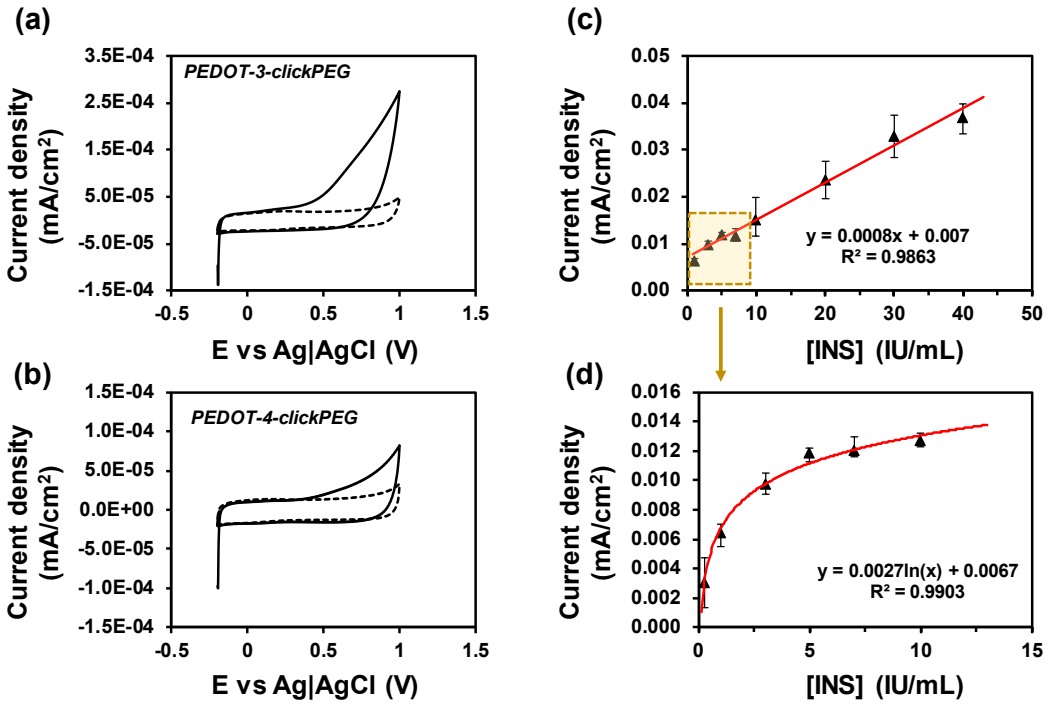

Figure 4. Electrochemical characterization of PEDOT-#-clickPEG hydrogels. Representative 3rd CV curve for (**a**) PEDOT-3-clickPEG and (**b**) PEDOT-4-clickPEG hydrogels. Dashed line corresponds to the blank hydrogel system (no PEDOT; 3-clickPEG or 4-clickPEG, respectively). Calibration plot of oxidation peak current vs. INS concentration considering an interval up to (**c**) 40 IU/mL (the yellow rectangular indicates the data that is zoomed in (**d**) with an interval up to 10 IU/mL). Plots were obtained by CV using carbon SPE. Error bars represent standard deviations of three independent measurements.

To test the INS release through our PEDOT-#-clickPEG hydrogels, we configured the system according to the following two principles [12]: (1) changes in PEDOT···INS and counter-anion···INS electrostatic interactions according to the oxidation degree of PEDOT chains either retain INS within the NPs+INS layer or, on the contrary, facilitate its release towards the solution media through the PEDOT-#-PEG matrix; and (2) PEDOT NPs in the PEDOT-#-PEG matrix act as anchoring INS points depending on the electrochemical stimulus, thus slowing down the diffusion of INS.

Briefly, a mixture of PEDOT NPs and INS was stabilized in 0.1 M PBS and then drop-casted onto a screen-printed electrode (working electrode, WE) to yield a thin coating layer (NPs+INS). Once dried, the PEDOT-#-

clickPEG hydrogel was let to gel on top of it for 15 min before any release test, for which PBS was used as release media under a constant stimulation potential for 100 s per day during 3 days (n = 6). Three different trigger conditions were considered: a positive voltage (+0.6 V), a negative voltage (−0.6 V), and no voltage. Every 24 h, media was collected before and after the stimulation event and replaced, with INS concentration being determined by CV after obtaining the corresponding calibration curves (Figure 4c,d).

Figure 5 shows the INS delivery profiles from NPs+INS/PEDOT-3-clickPEG and NPs+INS/PEDOT-4-clickPEG hydrogels considering a constant positive voltage of (+0.6 V) and a constant negative voltage (−0.6 V) as electrical stimuli as well as the non-stimulated condition. For the NPs+INS/PEDOT-4-clickPEG system, the application of a positive voltage effectively triggered INS release, while a negative voltage significantly suppressed it. In the absence of electrical stimulation, an accumulative INS release of 60% ± 5.5% of the total INS loaded on the hydrogel was determined. Upon applying a positive voltage, INS release increased by approximately 70% relative to the control, reaching 102% ± 8.0%, while a negative voltage reduced INS release by about 39%, down to 37% ± 4.1% (Figure 5a,b).

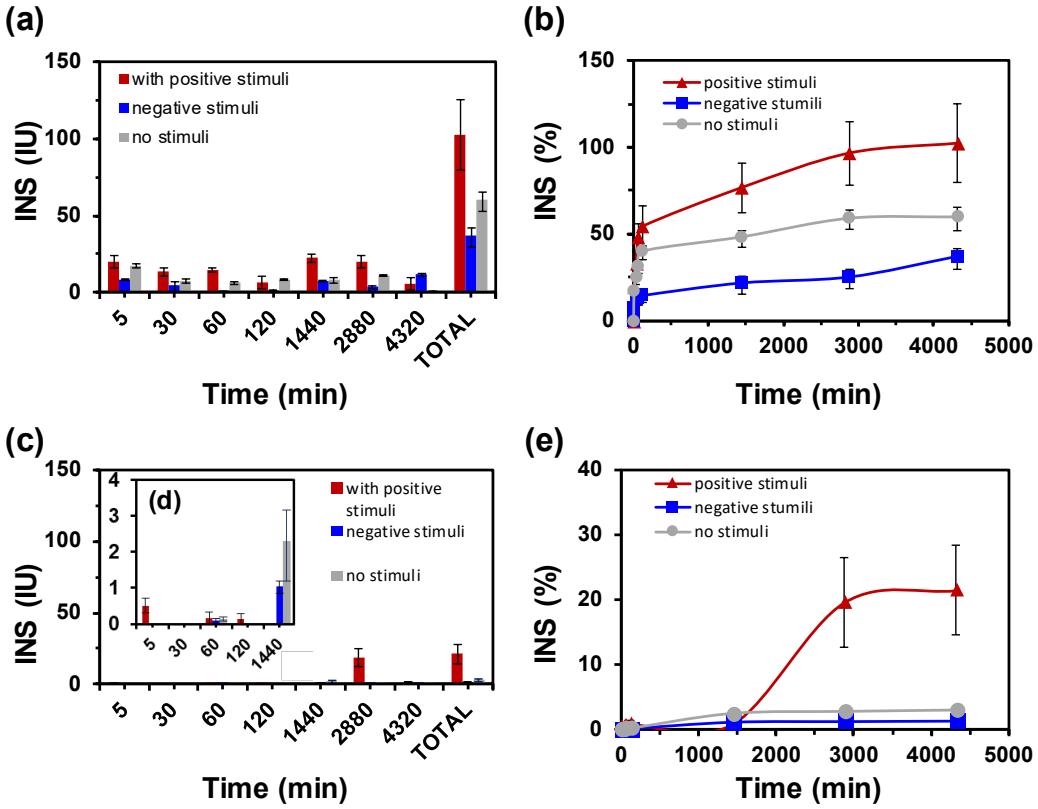

Figure 5. INS release profiles from (**a**,**b**) NPs-INS/PEDOT-4-clickPEG and (**c**,**d**) NPs-INS/PEDOT-3-clickPEG hydrogels under different electrical stimuli. Graphs (**a**,**c**,**d**) show INS release measured independently at specific time intervals, while (**b**,**e**) represent the cumulative INS release over time as a percentage of the total INS initially loaded into the devices. Panel (**d**), as an inset, shows the data from 0 to 1140 min with the y-scale (INS, IU) adjusted.

A similar trend was observed for the NPs+INS/PEDOT-3-clickPEG system, though with a markedly lower dynamic range. Under positive stimulation, INS release increased from 2.92% ± 0.78% to 21.38% ± 6.54%, while negative stimulation reduced it down to 1.31% ± 0.36% (Figure 5c,d). Thus, although both systems respond directionally in the same way—positive voltage enhancing and negative voltage reducing INS release -the 4-arm system exhibits a far greater absolute release capacity and tighter modulation, making it more suitable for precise, therapeutically relevant INS delivery.

The mechanism behind the electro-stimulated INS release is based on the electrostatic interaction between the protein, which is negatively charged at physiological pH, and the conducting polymer. The application of a positive voltage results in the creation of more positive charges along the PEDOT chains due to an oxidation process, which promotes the entrance of more counter-anions to compensate the overall charge. As a consequence, the electrostatic interactions between INS molecules and PEDOT chains are shielded by such new counterions while, at the same time, repulsive interactions between counter-anions and INS molecules are generated, thus

forcing INS to be released. Instead, when the applied voltage is negative, the positive charge of PEDOT chains decreases due to a reduction process and the excess of counter-anions are expelled from the PEDOT matrix to the medium. The latter decreases the amount of repulsive interaction between the counterions and the INS molecules, preventing its release.

It is important to note that the condition without stimulation applied is considered as a reference value that represents passive INS release. Accordingly, the characteristics of the PEDOT-#-clickPEG polymer matrix affect the diffusion of INS towards PBS. The observed differences between PEDOT-3-clickPEG and PEDOT-4-clickPEG hydrogels in terms of crosslinking density and, consequently, hydrophobicity (i.e., the thiol-yne crosslinking site is hydrophobic, which makes thiol-yne hydrogels nonswellable [33]) and elasticity of the PEG matrix, significantly hindered INS release without the possibility to electrochemically control its delivery. Although some degree of difference was expected between both systems, the low performance for PEDOT-3-clickPEG hydrogels and the impossibility to achieve smart control led us to discard it for the following tests. Hence, from now onwards, to evaluate the adequacy of our system in a biological context, for electrochemically controlled INS release, only PEDOT-4-clickPEG hydrogels will be considered.

The application of PEDOT-4-clickPEG hydrogels as biomaterials of choice in the design of devices for electrically-controlled INS delivery was evaluated from a tripartite perspective. First, the swelling kinetics of the thiol-yne PEG polymeric matrix system were evaluated. Then, its cytocompatibility was verified by means of indirect (lixiviates) and direct contact testing using mouse fibroblasts (L-929 cell line). Finally, the performance of NPs+INS/PEDOT-4-clickPEG system covered with a square piece of chicken skin was performed as an ex vivo test to monitor the INS delivery through a tissue-like barrier.

After immersion in an aqueous environment (PBS) at 37 °C, PEDOT-4-clickPEG hydrogels displayed a non-swelling profile with the increase in volume being controlled and under 100% for at least 25 days with no signs of bulk degradation (Figure 6a). Besides, PEDOT-4-clickPEG hydrogels exhibited favorable cytocompatibility, with relative cell viability of 86% ± 5% (Figure 6b,c). In addition, optical images of cells cultured for 72 h in direct contact with the conductive click-hydrogels displayed a healthy density and typical fibroblast-like morphology, with no signs of cell death or any inhibition halo effect being observed.

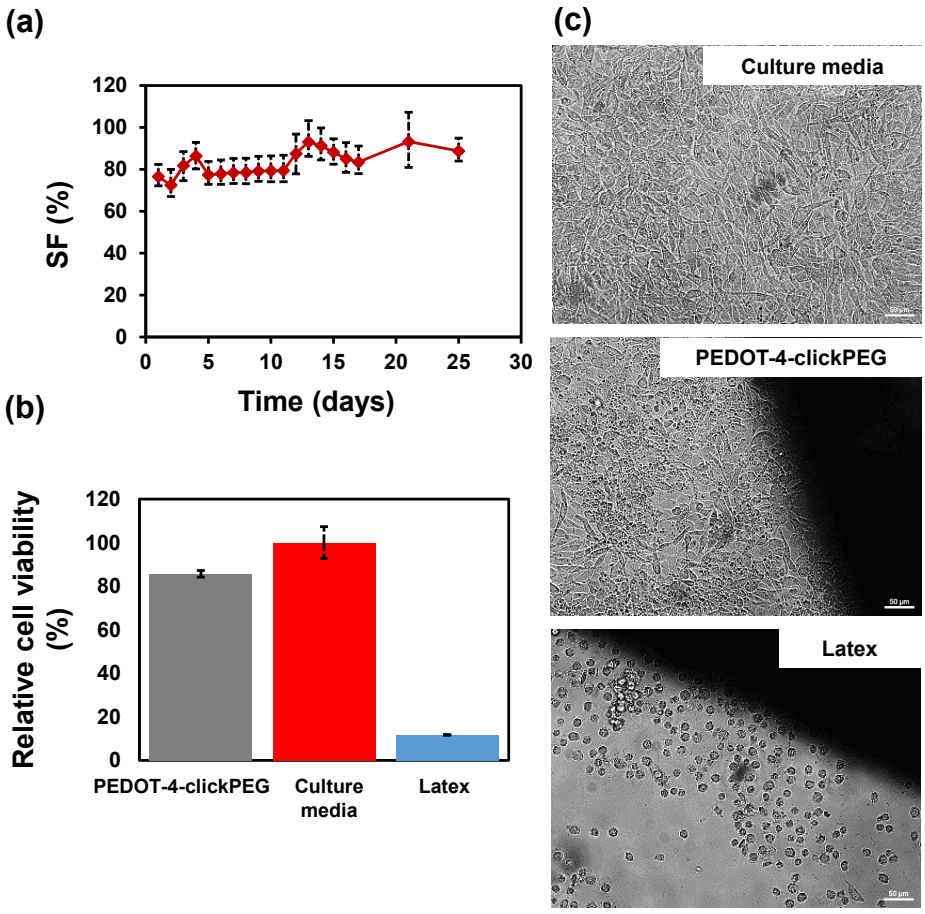

Figure 6. (**a**) Swelling kinetics of PEDOT-4-clickPEG hydrogels immersed in PBS and incubated at 37 °C in an orbital shaker incubator at 80 rpm. (**b**,**c**) Cytocompatibility of NPs+INS/PEDOT-4-clickPEG devices: (**b**) Relative

cell viability of L-929 mouse fibroblasts cultured in direct contact with the hydrogels, culture media or latex. (**c**) Optical images of L-929 cells cultured in direct contact with the tested systems.

After confirming the high cytocompatibility of PEDOT-4-clickPEG hydrogels, as well as its INS protective function, the INS delivery profile from NPs+INS/PEDOT-4-clickPEG through an ex vivo skin barrier was monitored following the same procedure as described above. Figure 7a displays a sketch of the set-up used during this experiment, while Figure 7b shows the absolute values of INS units released in PBS from NPs+INS/PEDOT-4-clickPEG devices (n = 6) in the ex vivo test at specific time intervals with a positive electrochemical stimulus applied (+0.6 V). As it can be observed, the values detected coincide with those obtained in the uncovered device under positive stimulus, which indicates how the presence of the skin barrier does not interfere with the electrically-stimulated release of INS and supports its application as injectable INS delivery platform.

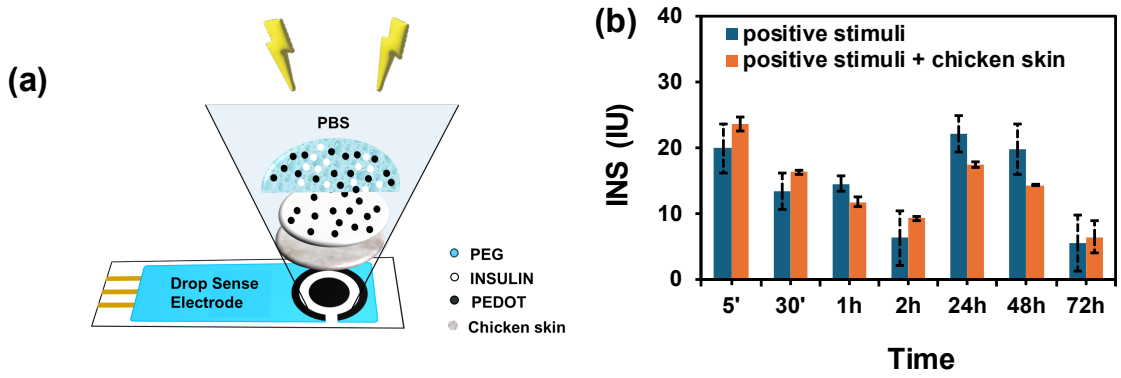

Figure 7. INS delivery from NPs+INS/PEDOT-4-clickPEG devices in an ex vivo testing: (**a**) Sketch for the set-up used; (**b**) INS units released from the devices (n = 6) at specific time points under a positive electrochemical stimulus (+0.6 V) in PBS.

Electro-regulated insulin delivery systems, which include implantable devices, transdermal patches, injectable systems, and hybrid/combined approaches [41], hold considerable promise for improving diabetes therapy by providing more precise, adaptable, and user-friendly ways of delivering insulin compared to traditional injections. Moreover, they offer the possibility of adaptive insulin delivery—moving closer to the goal of "artificial pancreas" systems. However, for real-world clinical implementation, the key will be proving long-term safety (biocompatibility and biodegradation/elimination), cost effectiveness (low manufacturing complexity and scalability), ease of use, and integration into patient care workflows. While the potential is high, most technologies are still at pre-clinical or early-clinical stages with several caveats apply to be solved, for instance safety concerns regarding device failure or electrical malfunction.

4. Conclusions

This study presents the design and thorough characterization of electroactive PEG-based click-hydrogels incorporating PEDOT NPs (PEDOT-#-clickPEG) for the electrochemically controlled delivery of INS. PEG precursors with different architecture (3-arm or 4-arm) were functionalized with thiol or alkyne terminal groups, and the resulting click-hydrogels derived from their combination compared in terms of gelation, mechanical behavior, porosity, electrochemical response, and INS release efficiency. PEDOT-4-clickPEG exhibited faster gelation (41% faster) and higher porosity than its 3-arm counterpart. Besides, by means of frequency sweeps, we confirmed mechanical stability in both systems, with PEDOT-3-clickPEG being stiffer (G′: 12.1 ± 1.8 kPa vs. 5.5 ± 1.1 kPa). Cyclic voltammetry validated the electroactivity of both hydrogels, enabling redox-driven INS release. When PEDOT-4-clickPEG was used, positive voltage (+0.6 V) increased INS release by ~70% relative to passive conditions, while negative stimulation (−0.6 V) suppressed its release by ~39%. In contrast, PEDOT-3-clickPEG showed a comparable directional response but with much lower dynamic range. Hence, only PEDOT-4-clickPEG achieved therapeutically relevant and controllable release, attributable to its lower crosslinking density and higher porosity. Additionally, PEDOT-4-clickPEG hydrogels showed minimal swelling for 25 days in PBS at 37 °C, excellent cytocompatibility with 86% ± 5% viability of L-929 fibroblasts, and preserved function in an ex vivo model using chicken skin as a barrier. Importantly, INS release under stimulation remained consistent with barrier-free conditions, confirming the feasibility of transdermal electrical stimulation. Altogether, PEDOT-4-clickPEG

hydrogels represent a promising platform for integration into closed-loop, sensor-guided systems for diabetes management, offering precise temporal control via externally applied electrical inputs.

Author Contributions

H.M.-G.: investigation, visualization, formal analysis, writing—review and editing; J.C.S.: investigation, validation, supervision, writing—review and editing; T.E.: validation, supervision, writing—review and editing; O.B.: software, writing—review and editing; F.C.F.: funding acquisition, writing—review and editing; A.E.-N.: investigation, validation, writing—review and editing; M.-P.G.: funding acquisition, writing—review and editing; C.A.: supervision, project administration, funding acquisition, writing—review and editing; M.M.P.-M.: formal analysis, validation, supervision, project administration, funding acquisition, writing—original draft preparation, writing—review and editing. All authors have read and agreed to the published version of the manuscript.

Funding

This publication is part of the I+D+i project PID2021-125767OB-I00 funded by MCIN/AEI/10.13039/501100011033 and, as appropriate, by "ERDF A way of making Europe", by the European Union. H. M.-G. thanks the Generalitat de Catalunya for a FI-SDUR 2020 Fellowship. This work is part of the Maria de Maeztu Units of Excellence Program No. CEX2023-001300-M funded by MCIN/AEI (10.13039/501100011033). M.M.P.-M. thanks the Spanish Ministry for the Junior Beatriz Galindo Award (BG20/00216). The authors are thankful to the Agència de Gestió d'Ajuts Universitaris i de Recerca (2021 SGR 00387 for H.M.-G., M.M.P.-M. and C.A. and 2021 SGR 01368 for A.E.-N. and M.-P.G.) for financial support. Support for the research of C.A. and M.-P.G. was also received through the prize "ICREA Academia" for excellence in research funded by the Generalitat de Catalunya. The authors also acknowledge funding from the FCT—"Fundação para a Ciência e Tecnologia" through the projects InSilico4OCReg (PTDC/EME-SIS/4446/2020) and eOnco (2022.07252.PTDC), and through institutional funds to iBB (UIDB/04565/2020 and UIDP/04565/2020) and to Associate Laboratory i4HB (LA/P/0140/2020).

Data Availability Statement

The data that support the findings of this study are available on request from the corresponding author M.M.P.-M.

Conflicts of Interest

The authors declare no conflict of interest.

Use of AI and AI-Assisted Technologies

No AI tools were utilized for this paper.

References

1. Benjamin, E. Designing a Closed-Loop Automated Insulin Delivery System: Simplifying Life for People, Including Children, Living with Type 1 Diabetes. *IEEE Pulse* **2024**, *15*, 5–10. https://doi.org/10.1109/MPULS.2024.3443488.
2. Diem, P.; Ducluzeau, P.H.; Scheen, A. The Discovery of Insulin. *Diabetes Epidemiol. Manag.* **2022**, *5*, 100049. https://doi.org/10.1016/j.deman.2021.100049.
3. Sims, E.K.; Carr, A.L.J.; Oram, R.A.; et al. 100 Years of Insulin: Celebrating the Past, Present and Future of Diabetes Therapy. *Nat. Med.* **2021**, *27*, 1154–1164. https://doi.org/10.1038/s41591-021-01418-2.
4. American Diabetes Association Professional Practice Committee. 6. Glycemic Goals and Hypoglycemia: Standards of Care in Diabetes-2024. *Diabetes Care* **2024**, *47* (Suppl. 1), S111–S125. https://doi.org/10.2337/dc24-S006.
5. Zhang, X.; Chen, G.; Zhang, H.; et al. Bioinspired Oral Delivery Devices. *Nat. Rev. Bioeng.* **2023**, *1*, 208–225. https://doi.org/10.1038/s44222-022-00006-4.
6. Lou, J.; Duan, H.; Qin, Q.; et al. Advances in Oral Drug Delivery Systems: Challenges and Opportunities. *Pharmaceutics* **2023**, *15*, 484. https://doi.org/10.3390/pharmaceutics15020484.
7. Wang, T.; Shen, L.; Zhang, Y.; et al. "Oil-Soluble" Reversed Lipid Nanoparticles for Oral Insulin Delivery. *J. Nanobiotechnol.* **2020**, *18*, 98. https://doi.org/10.1186/s12951-020-00657-8.
8. Li, H.; Shi, Y.; Ding, X.; et al. Recent Advances in Transdermal Insulin Delivery Technology: A Review. *Int. J. Biol. Macromol.* **2024**, *274*, 133452. https://doi.org/10.1016/j.ijbiomac.2024.133452.

9. Niloy, K.K.; Lowe, T.L. Injectable systems for long-lasting insulin therapy. *Adv. Drug Delivery Rev.* **2023**, *203*, 115121. https://doi.org/10.1016/j.addr.2023.115121.
10. Gill, H.S.; Denson, D.D.; Burris, B.A.; et al. Effect of Microneedle Design on Pain in Human Volunteers. *Clin. J. Pain* **2008**, *24*, 585–594. https://doi.org/10.1097/AJP.0b013e31816778f9.
11. Li, C.; Wan, L.; Luo, J.; et al. Advances in Subcutaneous Delivery Systems of Biomacromolecular Agents for Diabetes Treatment. *Int. J. Nanomed.* **2021**, *16*, 1261–1280. https://doi.org/10.2147/IJN.S283416.
12. Dhote, V. Iontophoresis: A Potential Emergence of a Transdermal Drug Delivery System. *Sci. Pharm.* **2012**, *80*, 1–28. https://doi.org/10.3797/scipharm.1108-20.
13. Bakshi, P.; Vora, D.; Hemmady, K.; et al. Iontophoretic Skin Delivery Systems: Success and Failures. *Int. J. Pharm.* **2020**, *586*, 119584. https://doi.org/10.1016/j.ijpharm.2020.119584.
14. Park, S.-B.; Ko, J.; Kim, J.-U.; et al. Transdermal Insulin Delivery for Type 1 Diabetes Using Reverse Electrodialysis and Ionic Liquid Technology Based on a Size-Dependent Protein Delivery Study. *ACS Appl. Nano Mater.* **2025**, *8*, 6509–6518. https://doi.org/10.1021/acsanm.5c00177.
15. Kim, K.-J.; Yun, Y.-H.; Je, J.-Y.; et al. Photothermally Controlled Drug Release of Naproxen-Incorporated Mungbean Starch/PVA Biomaterials Adding Melanin Nanoparticles. *Process Biochem.* **2023**, *129*, 268–280. https://doi.org/10.1016/j.procbio.2023.03.034.
16. Ogura, M.; Paliwal, S.; Mitragotri, S. Low-Frequency Sonophoresis: Current Status and Future Prospects. *Adv. Drug Deliv. Rev.* **2008**, *60*, 1218–1223. https://doi.org/10.1016/j.addr.2008.03.006.
17. Ramadon, D.; McCrudden, M.T.C.; Courtenay, A.J.; et al. Enhancement Strategies for Transdermal Drug Delivery Systems: Current Trends and Applications. *Drug Deliv. Transl. Res.* **2022**, *12*, 758–791. https://doi.org/10.1007/s13346-021-00909-6.
18. Cha, H.J.; He, C.; Zhao, H.; et al. Intercellular and Intracellular Functions of Ceramides and Their Metabolites in Skin (Review). *Int. J. Mol. Med.* **2016**, *38*, 16–22. https://doi.org/10.3892/ijmm.2016.2600.
19. Mazhar, D.; Haq, N.U.; Zeeshan, M.; et al. Preparation, Characterization, and Pharmacokinetic Assessment of Metformin HCl Loaded Transfersomes Co-Equipped with Permeation Enhancer to Improve Drug Bioavailability via Transdermal Route. *J. Drug Deliv. Sci. Technol.* **2023**, *84*, 104448. https://doi.org/10.1016/j.jddst.2023.104448.
20. Sidat, Z.; Marimuthu, T.; Kumar, P.; et al. Ionic Liquids as Potential and Synergistic Permeation Enhancers for Transdermal Drug Delivery. *Pharmaceutics* **2019**, *11*, 96. https://doi.org/10.3390/pharmaceutics11020096.
21. Islam, M.R.; Uddin, S.; Chowdhury, M.R.; et al. Insulin Transdermal Delivery System for Diabetes Treatment Using a Biocompatible Ionic Liquid-Based Microemulsion. *ACS Appl. Mater. Interfaces* **2021**, *13*, 42461–42472. https://doi.org/10.1021/acsami.1c11533.
22. Zou, J.-J.; Le, J.-Q.; Zhang, B.-C.; et al. Accelerating Transdermal Delivery of Insulin by Ginsenoside Nanoparticles with Unique Permeability. *Int. J. Pharm.* **2021**, *605*, 120784. https://doi.org/10.1016/j.ijpharm.2021.120784.
23. Sugumar, V.; Hayyan, M.; Madhavan, P.; et al. Current Development of Chemical Penetration Enhancers for Transdermal Insulin Delivery. *Biomedicines* **2023**, *11*, 664. https://doi.org/10.3390/biomedicines11030664.
24. Nabila, F.H.; Islam, R.; Yamin, L.; et al. Transdermal Insulin Delivery Using Ionic Liquid-Mediated Nanovesicles for Diabetes Treatment. *ACS Biomater. Sci. Eng.* **2025**, *11*, 402–414. https://doi.org/10.1021/acsbiomaterials.4c02000.
25. Daly, A.B.; Boughton, C.K.; Nwokolo, M.; et al. Fully Automated Closed-Loop Insulin Delivery in Adults with Type 2 Diabetes: An Open-Label, Single-Center, Randomized Crossover Trial. *Nat. Med.* **2023**, *29*, 203–208.
26. Sabbagh, F.; Muhamad, I.I.; Niazmand, R.; et al. Recent Progress in Polymeric Non-Invasive Insulin Delivery. *Int. J. Biol. Macromol.* **2022**, *203*, 222–243. https://doi.org/10.1016/j.ijbiomac.2022.01.134.
27. Vargas, E.; Nandhakumar, P.; Ding, S.; et al. Insulin Detection in Diabetes Mellitus: Challenges and New Prospects. *Nat. Rev. Endocrinol.* **2023**, *19*, 487–495. https://doi.org/10.1038/s41574-023-00842-3.
28. Zhao, P.; Liu, Y.; Xiao, L.; et al. Electrochemical Deposition to Construct a Nature Inspired Multilayer Chitosan/Layered Double Hydroxides Hybrid Gel for Stimuli Responsive Release of Protein. *J. Mater. Chem. B* **2015**, *3*, 7577–7584. https://doi.org/10.1039/C5TB01056J.
29. Zhao, X.; Xue, W.; Ding, W.; et al. A Novel Injectable Sodium Alginate/Chitosan/Sulfated Bacterial Cellulose Hydrogel as Biohybrid Artificial Pancreas for Real-Time Glycaemic Regulation. *Carbohydr. Polym.* **2025**, *354*, 123323. https://doi.org/10.1016/j.carbpol.2025.123323.
30. Ali, A.; Saroj, S.; Saha, S.; et al. Glucose-Responsive Chitosan Nanoparticle/Poly(Vinyl Alcohol) Hydrogels for Sustained Insulin Release In Vivo. *ACS Appl. Mater. Interfaces* **2023**, *15*, 32240–32250. https://doi.org/10.1021/acsami.3c05031.
31. Wang, Y.; Yu, H.; Wang, L.; et al. Microneedles with Two-Stage Glucose-Sensitive Controlled Release for Long-Term Insulin Delivery. *ACS Biomater. Sci. Eng.* **2023**, *9*, 2534–2544. https://doi.org/10.1021/acsbiomaterials.3c00137.
32. Mallawarachchi, S.; Mahadevan, A.; Gejji, V.; et al. Mechanics of Controlled Release of Insulin Entrapped in Polyacrylic Acid Gels via Variable Electrical Stimuli. *Drug Deliv. Transl. Res.* **2019**, *9*, 783–794. https://doi.org/10.1007/s13346-019-00620-7.

33. Muñoz-Galán, H.; Molina, B.G.; Bertran, O.; et al. Combining Rapid and Sustained Insulin Release from Conducting Hydrogels for Glycemic Control. *Eur. Polym. J.* **2022**, *181*, 111670. https://doi.org/10.1016/j.eurpolymj.2022.111670.
34. Muñoz-Galán, H.; Enshaei, H.; Silva, J.C.; et al. Electroresponsive Thiol–Yne Click-Hydrogels for Insulin Smart Delivery: Tackling Sustained Release and Leakage Control. *ACS Appl. Polym. Mater.* **2024**, *6*, 8093–8104. https://doi.org/10.1021/acsapm.4c00911.
35. Macdougall, L.J.; Pérez-Madrigal, M.M.; Arno, M.C.; et al. Nonswelling Thiol–Yne Cross-Linked Hydrogel Materials as Cytocompatible Soft Tissue Scaffolds. *Biomacromolecules* **2018**, *19*, 1378–1388. https://doi.org/10.1021/acs.biomac.7b01204.
36. Resina, L.; El Hauadi, K.; Sans, J.; et al. Electroresponsive and PH-Sensitive Hydrogel as Carrier for Controlled Chloramphenicol Release. *Biomacromolecules* **2023**, *24*, 1432–1444. https://doi.org/10.1021/acs.biomac.2c01442.
37. Phillips, J.C.; Braun, R.; Wang, W.; et al. Scalable Molecular Dynamics with NAMD. *J. Comput. Chem.* **2005**, *26*, 1781–1802. https://doi.org/10.1002/jcc.20289.
38. Muñoz-Galán, H.; Marzoa, A.; Bertran, O.; et al. Optomechanical, Computer Simulation, and Nanoindentation Studies on Tunable Click Hydrogels: Microscopic Insights. *ACS Appl. Polym. Mater.* **2024**, *6*, 12176–12185. https://doi.org/10.1021/acsapm.4c02250.
39. UNE-EN ISO 10993-5:2009; Biological evaluation of medical devices—Part 5: Tests for in vitro cytotoxicity. Aenor: Madrid, Spain, 2009.
40. Baruah, S.; Mohanta, D.; Betty, C.A. Composite PEDOT-PSS Based Highly Sensitive Electrochemical Sensors for Sensing Glucose from Human Saliva. *Microchem. J.* **2024**, *206*, 111411. https://doi.org/10.1016/j.microc.2024.111411.
41. Alemán, C.; Muñoz-Galán, H.; Pérez-Madrigal, M.M. Recent Advances in Electrically Stimulated Insulin Delivery Systems. *ACS Omega* **2025**, *10*, 40750–40768. https://doi.org/10.1021/acsomega.5c06147.